JJEE
Volume 1, Number 2, 2015
Pages 93-109
Jordan Journal of Electrical Engineering
ISSN (Print): 2409-9600, ISSN (Online): 2409-9619

A Radon-Slantlet Multi-Carrier Code Division Multiple Access Transceiver Design and Simulation under Different Channel Conditions

Abbas H. Kattoush

Department of Communications & Electronics Engineering, Al-Ahliyya Amman University, Amman, Jordan
e-mail: akattoush@yahoo.ca

Received: May 8, 2015 *Accepted: July 4, 2015*

Abstract— Wireless digital communication networks are rapidly expanding resulting in a demand for reliable and high spectral efficiency systems. Multi-Carrier Code Division Multiple Access (MC-CDMA) has emerged recently as a promising candidate for the next generation broad-band mobile networks. It was found that Radon based orthogonal frequency division multiplexing (OFDM) and discrete Slantlet transform (SLT) based OFDM are capable of reducing inter symbol interference (ISI) and inter carrier interference (ICI), which are caused by the loss of orthogonality between the carriers. Radon-based OFDM and SLT-based OFDM can also support much higher spectrum efficiency than fast Fourier transform-based OFDM (FFT-OFDM). In this paper, a novel Radon-SLT-MC-CDMA transceiver design will be presented based on a new design of a Radon-SLT-OFDM that is used as a basic building block in the design of MC-CDMA transceiver to increase orthogonality against the multi-path frequency selective fading channels. Simulation results are provided to demonstrate the significant gains in performance due to the proposed technique. The bit error rate (BER) performance of the proposed Radon-SLT-MC-CDMA scheme was compared with that of FFT based MC-CDMA, Radon based MC-CDMA, and discrete Multiwavelet transform (DMWT) based MC-CDMA and tested in additive white Gaussian noise (AWGN), Flat fading and Selective fading channels. The simulation results showed that the proposed system outperforms the other three systems.

Keywords— FFT based MC-CDMA, finite Radon transform, multiwavelet based MC-CDMA, Radon-SLT based OFDM, Radon based MC-CDMA, slantlet Transform.

I. INTRODUCTION

Multi-path fading channels have a severe effect on the performance of wireless communication systems especially those systems that exhibit efficient bandwidth, like OFDM and MC-CDMA. There is always a need for developments in the realization of these systems as well as efficient channel estimation and equalization methods to enable these systems to reach their maximum performance [1].

CDMA has been a strong candidate to support multimedia mobile services because it has the ability to cope with the asynchronous nature of the multimedia traffic; and it can provide higher capacity as opposed to the conventional access schemes [2]-[3]. The main problem in the design of a communication system over a wireless link is to deal with multi-path fading, which causes a significant degradation in terms of both the reliability of the link and the data rate [4].

In the last two decades, a number of MC-CDMA systems have been proposed as an alternative to the classical single-carrier CDMA systems [5]-[9]. The principle of CDMA was combined with FFT-OFDM which allows one to use the available spectrum in an efficient way and retain the many advantages of a CDMA system. This combination of OFDM-CDMA or Multi-Carrier CDMA was first proposed in [10]. It is a useful technique for four generation (4G) systems where variable data rates as well as reliable communication systems are needed. Combining OFDM with CDMA has one major advantage; it can lower the symbol rate in

Corresponding author's e-mail: akattoush@yahoo.ca

each subcarrier compared to OFDM, so that longer symbol duration makes it easier to synchronize. MC-CDMA not only mitigates the ISI but also exploits the multipath.

To combat ISI and ICI, cyclic prefix (CP) is inserted between FFT-OFDM symbols which take around 25 percent of bandwidth. To improve bandwidth efficiency and reduce ISI and ICI, discrete wavelet transform (DWT) based OFDM is proposed. In [11], the conventional Fourier based complex exponential carriers of the OFDM system is replaced with some orthonormal wavelets in order to reduce the level of interference. The wavelets are derived from multistage tree-structured Haar and Daubechies orthonormal quadrature mirror filter bank. Compared with the conventional OFDM, it was found that the Haar and Daubechies-based orthonormal wavelets are capable of reducing the power of ISI and ICI.

Recently, Selesnick [12] has constructed a new orthogonal discrete wavelet transform. The slantlet transform has two zero moments and improved time localization [13]. Due to a very high spectral containment property of wavelet filters, SLT transform can be used as a main building block in designing an improved spectral efficiency OFDM system where the SLT modulator replaces the FFT modulator. SLT-based OFDM can better combat narrowband interferences and robust to ICI than traditional FFT filters [14]. Moreover, since the classic notion of a guard band does not apply for SLT-OFDM, data rates can be enhanced over those of FFT implementations [15].

In order to further reduce the level of interference, increase orthogonality and increase spectral efficiency, this paper implements a Radon mapper in SLT-OFDM instead of quadrature amplitude modulation (QAM) mapper and proposes a new design for a Radon-SLT-MC-CDMA system. The new design is studied and compared with FFT-MC-CDMA, Radon-FFT-MC-CDMA, and DMWT-MC-CDMA, on three different channel models: AWGN, flat fading and selective fading. Simulation results show that the proposed design achieves much lower bit error rates, increases signal to noise power ratio (SNR), and can be used as an alternative to the conventional MC-CDMA.

II. MC-CDMA SYSTEM

The MC-CDMA transmitter spreads the original data stream over different subcarriers using a given spreading code in the frequency domain [10]. Fig. 1 and Fig. 2 show the MC-CDMA transmitter of the k_{th} user for BPSK scheme and the power spectrum of the transmitted signal respectively [6], where $d_k(t)$ is the data bits for k_{th} user, G_{MC} denotes the processing gain, N_C is the number of subcarriers and $c_k(t) = [c_k^1 c_k^2 \cdots c_k^{G_{MC}}]$ is the spreading Pseudo-random Noise (PN) sequence of the k_{th} user. It is assumed that $N_C = G_{MC}$ as in [10]. However, N_C does not have to be equal to G_{MC} as in [6].

In MC-CDMA systems, the original data stream from a user is spread with the user's specific spreading code in the frequency domain. In other words, a fraction of the symbol corresponding to a chip of the spreading code is transmitted through a different subcarrier [15]. The narrowband subcarriers are generated using BPSK modulated signals, each at different frequencies, which at baseband are multiples of a harmonic frequency $1/T_S$. That is

$$\Delta f = f_i - f_{i-1} = 1/T_S \tag{1}$$

where T_S is the symbol duration of the data stream. The subcarrier frequencies are orthogonal to each other at baseband. The transmitted signal of the k_{th} user is given by

$$S_k^{MC}(t) = d_k(t)\sum_{i=1}^{N_C} c_k^i \cos\omega_i t \tag{2}$$

and the total bandwidth required for transmission is $(N_C+1)G_{MC}/N_C T_S$.

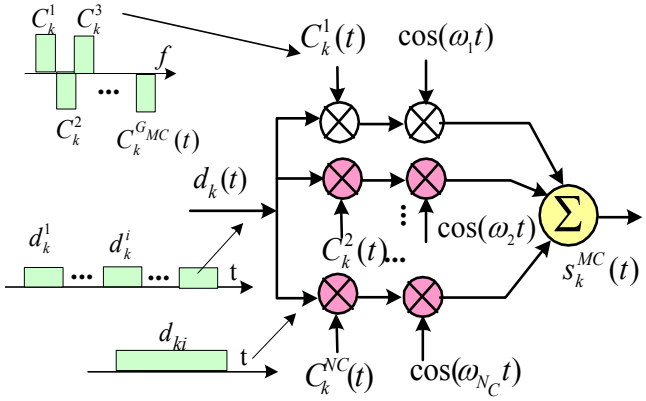

Fig. 1. MC-CDMA transmitter system model

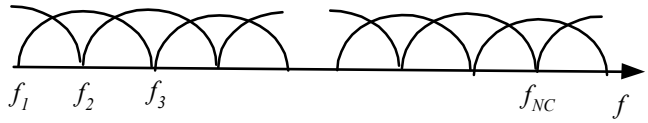

Fig. 2. Power spectrum representation of the transmitted signal

Fig. 3 shows the receiver of MC-CDMA systems [6]. The received signal $r(t)$ for all *K* users is given as

$$r(t) = \sum_{k=1}^{K} d_k(t)\sum_{i=1}^{N_C} h(i)c_k^i \cos\omega_i t + n(t) \tag{3}$$

where *n(t)* is the Additive White Gaussian Noise (AWGN) and *h(i)* is the complex signal channel coefficient of the i_{th} subcarrier. The received signal is demodulated with a corresponding subcarrier followed by lowpass filtering to generate the baseband signal. The baseband signal is weighted by coefficients $\{q_i, i = 1,2,...,G_{MC}\}$ and then all baseband signals are combined together. From Fig. 3, it can be seen that the received signal is combined in the frequency domain, so that the receiver can always employ all the received signal energy scattered in the frequency domain. This is the advantage of MC-CDMA [10]-[15]. Different combining techniques, which correspond to different choices of $\{q_i, i = 1,2,...,G_{MC}\}$ can be used to enhance system performance. Typical combining techniques include maximum ratio combining, equal gain combining [10] and minimum mean square error combining. The drawback of this system is that it does not consider the multipath and fading effects.

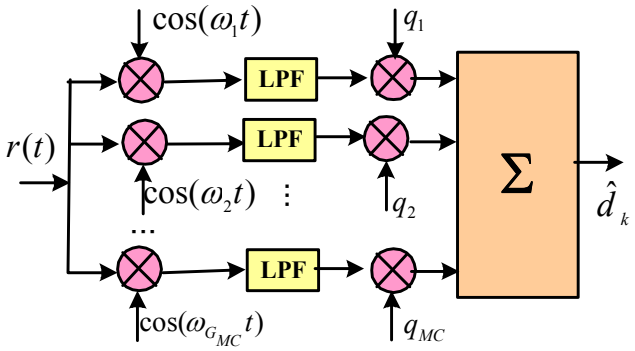

Fig. 3. MC-CDMA receiver system model

III. THE RADON-SLANTLET BASED OFDM TRANSCEIVER

The block diagram of SLT-OFDM is shown in Fig. 4. The main and important difference between FFT-OFDM and SLT-OFDM is that in SLT-OFDM the cyclic prefix (CP), which is usually 40% of the length of the frame, is not added to OFDM symbols [14]. Therefore, data rates in SLT-OFDM are higher than those of the FFT-OFDM.

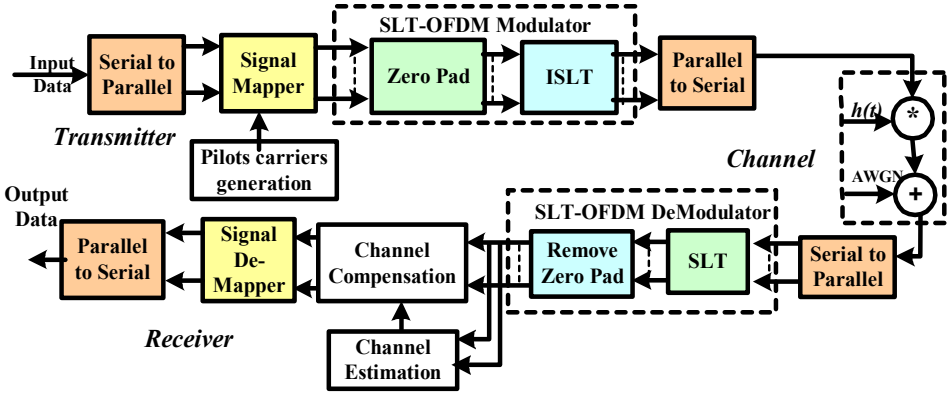

Fig. 4. Block diagram of SLT-OFDM system

Recently several models of Radon mappers were proposed to replace QAM mappers in OFDM transceivers [16]-[22]. As a result of applying FRAT, the bit error rate (BER) performance is improved significantly especially in the existence of multi-path fading channels. Also, it was found that Radon-based OFDM structure is less sensitive to channel parameters variation, like maximum delay, path gain, and maximum Doppler shift in selective fading channels as compared with standard OFDM structure. In Radon based OFDM system, FRAT mapping is used instead of QAM mapping; and the other processing parts of the system remain the same as in conventional QAM OFDM system [18].

The Radon-SLT-OFDM is actually a SLT-OFDM with a Radon mapper replacing QAM-mapper; the other processing parts of the system remain the same as in SLT-OFDM system [23]. The processes of serial to parallel (S/P) converter, signal demapper, insertion of training sequence, and zero padding operation are the same as in the SLT-OFDM. After that, the ISLT is applied to the signal. At the receiver, the zeros padded at the transmitter are removed; and the other operations of channel estimation, channel compensation, signal demapping and parallel to serial (P/S) conversion are performed in the same manner as in FFT based OFDM.

A. Radon Data Mapping–Demapping Algorithm

In conventional FFT-OFDM system, the length of input data frame is 60 symbols, and in Radon-SLT OFDM system, the length of the input data frame must be $(p \times p)$, where p is a prime number. The closest number to 60 is (7×7) which makes the frame length 49 symbols. This is because the input of FRAT must be a two dimensional matrix with size $(p \times p)$. The algorithm of one dimensional Radon mapping was first proposed in [17] and it is as follows:
Suppose $d(k)$ is the serial data stream to be transmitted using OFDM modulation scheme. Converting $d(k)$ from serial form to parallel form will construct a one dimensional vector containing the data symbols to be transmitted,

$$d(k) = (d_0\ d_1\ d_2\ .....\ d_n)^T \tag{4}$$

where k and n are the time index and the vector length respectively. Then convert the data packet represented by the vector $d(k)$ from one-dimensional vector to a $p \times p$ two dimensional matrix $D(k)$, where p should be a prime number according to the matrix resize operation.
Take the 2-D FFT of the matrix $D(k)$ to obtain the matrix, $\mathcal{F}(r,s)$. For simplicity it will be labeled by $\mathcal{F}$:

$$\mathcal{F}(r,s) = \sum_{m=0}^{p-1}\sum_{n=0}^{p-1} D(m,n) e^{-j(2\pi/p)rm} e^{-j(2\pi/p)ns} \tag{5}$$

Redistribute the elements of the matrix $\mathcal{F}$ according to the following optimum ordering algorithm first described in [24]. The optimum number of FRAT projections is one projection for each column; and the best ordering of the 2D-FFT coefficients in these projections can be achieved if the normal vectors are determined as [24]:

$$\begin{aligned} (a_k, b_k) = \arg \quad & \min \quad \left| (C_p(a_k), C_p(b_k)) \right| \\ & (a_k, b_k) \in \{n\,u_k : 1 \le n \le p-1\} \\ & st.\ \ C_p(b_k) \ge 0 \end{aligned} \tag{6}$$

Here $C_p(x)$ denotes the centralized function of period p ; $C_p(x) = x - p.round(x/p)$. Hence, $\|(C_p(a_k), C_p(b_k))\|$ represents the distance from the origin to the point (a_k, b_k) on the Fourier plane. The constraint $C_p(b_k) \ge 0$ is imposed in order to remove the ambiguity in deciding between (a,b) and $(-a,-b)$ as the normal vector for the projection. As a result, the optimal normal vectors are restricted to have angles in $(0,\pi)$. So, the dimensions of the resultant matrix will be $p \times (p+1)$ and will be denoted by the symbol $\mathcal{F}_{opt}$.

Take the 1D-IFFT for each column of the matrix $\mathcal{F}_{opt}$ to obtain the matrix of Radon coefficients $\mathbf{R}$:

$$\mathbf{R} = \frac{1}{p}\sum_{k=0}^{N-1} \mathcal{F}_{opt}\, e^{(j2\pi kn/p)} \tag{7}$$

Construct the complex matrix $\overline{\mathbf{R}}$ from the real matrix $\mathbf{R}$ so that its dimensions will be $p \times (p+1)/2$ according to:

$$\overline{r_{l,m}} = r_{i,j} + j \quad r_{i,j+1}, \quad 1 \le i \le p, \quad 1 \le j \le p \tag{8}$$

where $\overline{r_{l,m}}$ refers to the elements of the matrix $\overline{\mathbf{R}}$, while $r_{i,j}$ refers to the elements of the matrix $\mathbf{R}$. The complex matrix construction is made for the purpose of increasing bit per Hertz of mapping before resizing the mapped data.

Resize the matrix $\overline{\mathbf{R}}$ to a one dimensional vector $\mathbf{r}(k)$ of length $p \times (p+1)/2$.

$$\mathbf{r}(k) = \left(r_0\ r_1\ r_2\ .....\ r_{p(p+1)/2}\right)^T \tag{9}$$

Take the 1D-IFFT for the vector $\mathbf{r}(k)$ to obtain the sub-channel modulation.

$$\mathbf{s}(n) = \frac{1}{p(p+1)/2}\sum_{k=0}^{N_C-1} r(k)\, e^{j2\pi kn/\left[p(p+1)/2\right]} \tag{10}$$

where N_C is the number of carriers.

Finally, convert the vector $\mathbf{s}(n)$ to serial data symbols: $s_0, s_1, s_2, \ldots, s_n$.

B. The Slantlet Transform

The slantlet transform was first proposed by Selesnick [12]. It is an orthogonal discrete wavelet transform (DWT) with two zero moments and with improved time localization. It uses a special case of a class of bases described by Alpert in [25], the construction of which relies on Gram–Schmidt orthogonalization. Unlike iterated filter-bank approaches for the DWT SLT is based on the principle of designing different filters for different scales. Selesnick described the basis from a filter-bank viewpoint, gave explicit solutions for filter coefficients and described an efficient algorithm for the transform.

The usual iterated DWT filter-bank and its equivalent form are shown in Fig. 5. The "slantlet" filter-bank is based on an equivalent structure occupied by different filters that are not products. With this extra degree of freedom obtained by giving up the product form, filters of shorter length are designed to satisfy orthogonality and zero moment conditions.

For two-channel case, the Daubechies filter [26] is the shortest filter which makes the filter-bank orthogonal and has K zero moments. For $K = 2$ zero moments, filters $H(z)$ and $F(z)$ are of length 4. For this system, the iterated filters in Fig. 5 are of length 10 and 4. Without the constraint of which the filters are products, an orthogonal filter-bank with $K = 2$ zero moments can be obtained, where the filter lengths are 8 and 4 as shown in Fig. 5. That is a reduction by two samples and a difference that grows with the number of stages. This reduction in length, while maintaining desirable orthogonality and moment properties, is

possible because these filters are not constrained by the product form arising in the case of iterated filter-banks.

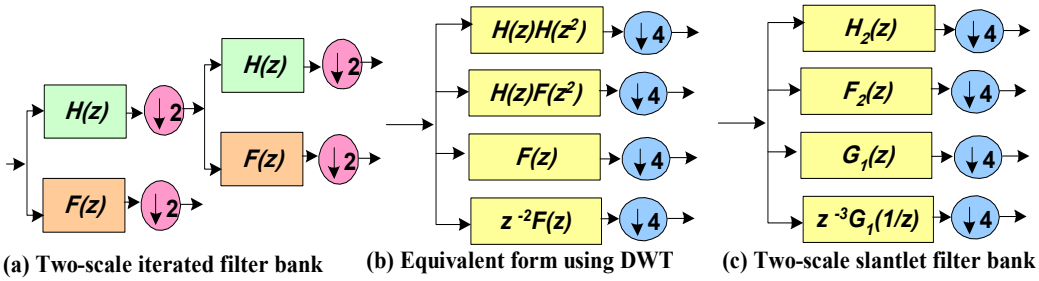

Fig. 5. Two-scale iterated filter-bank, its equivalent form using the DWT, and two-scale slantlet filter bank

Filters coefficients used in the SLT filter-bank as derived in [12] are given by:

$$G_1(z)=\left(-\frac{\sqrt{10}}{20}-\frac{\sqrt{2}}{4}\right)+\left(\frac{3\sqrt{10}}{20}+\frac{\sqrt{2}}{4}\right)z^{-1}+\left(-\frac{3\sqrt{10}}{20}+\frac{\sqrt{2}}{4}\right)z^{-2}+\left(\frac{\sqrt{10}}{20}-\frac{\sqrt{2}}{4}\right)z^{-3} \tag{11}$$

$$\begin{aligned}F_2(z)=&\left(\frac{7\sqrt{5}}{80}-\frac{3\sqrt{55}}{80}\right)+\left(-\frac{\sqrt{5}}{80}-\frac{\sqrt{55}}{80}\right)z^{-1}+\left(-\frac{9\sqrt{5}}{80}+\frac{\sqrt{55}}{80}\right)z^{-2}\\&+\left(-\frac{17\sqrt{5}}{80}+\frac{3\sqrt{55}}{80}\right)z^{-3}+\left(\frac{7\sqrt{5}}{80}+\frac{3\sqrt{55}}{80}\right)z^{-4}+\left(\frac{9\sqrt{5}}{80}+\frac{\sqrt{55}}{80}\right)z^{-5}\\&+\left(\frac{\sqrt{5}}{80}-\frac{\sqrt{55}}{80}\right)z^{-6}+\left(-\frac{7\sqrt{5}}{80}-\frac{3\sqrt{55}}{80}\right)z^{-7}\end{aligned} \tag{12}$$

$$\begin{aligned}H_2(z)=&\left(\frac{1}{16}+\frac{\sqrt{11}}{16}\right)+\left(\frac{3}{16}+\frac{\sqrt{11}}{16}\right)z^{-1}+\left(\frac{5}{16}+\frac{\sqrt{11}}{16}\right)z^{-2}\\&+\left(\frac{7}{16}+\frac{\sqrt{11}}{16}\right)z^{-3}+\left(\frac{7}{16}-\frac{\sqrt{11}}{16}\right)z^{-4}+\left(\frac{5}{16}-\frac{\sqrt{11}}{16}\right)z^{-5}\\&+\left(\frac{3}{16}-\frac{\sqrt{11}}{16}\right)z^{-6}+\left(\frac{1}{16}-\frac{\sqrt{11}}{16}\right)z^{-7}\end{aligned} \tag{13}$$

Slantlet filters are piecewise linear. Even though there is no tree structure for SLT, it can be efficiently implemented like an iterated DWT filter-bank [12]. Therefore, a computational complexity of the SLT is of the same order as that of the DWT.

IV. PROPOSED REALIZATION OF RADON-SLT-BASED MC-CDMA

The block diagram of the proposed system for Radon-SLT-MC-CDMA is depicted in Fig. 6. In this design, the QAM-FFT-OFDM is replaced by a Radon-SL-OFDM which does not require a cyclic prefix, has a better performance, has a higher data rates, and has a reduced ISI and ICI compared with FFT-based OFDM [23]. Each data symbol is multiplied with a spreading sequence. The gold sequence spreading code can be used since it has a relatively good correlation values. Other spreading codes that have a relatively good correlation values like Walsh-Hadamard (WH) code can be used when a small number of users are considered. The orthogonality of the code is reduced by the multipath propagation [27]. If FRAT ia

applied as a signal mapper in the proposed system, the length of the Gold sequence must be $(p \times p)$ such as (9, 25, and 49), where p is a prime number. This is because the input of FRAT must be a two dimensional matrix with size $(p \times p)$.

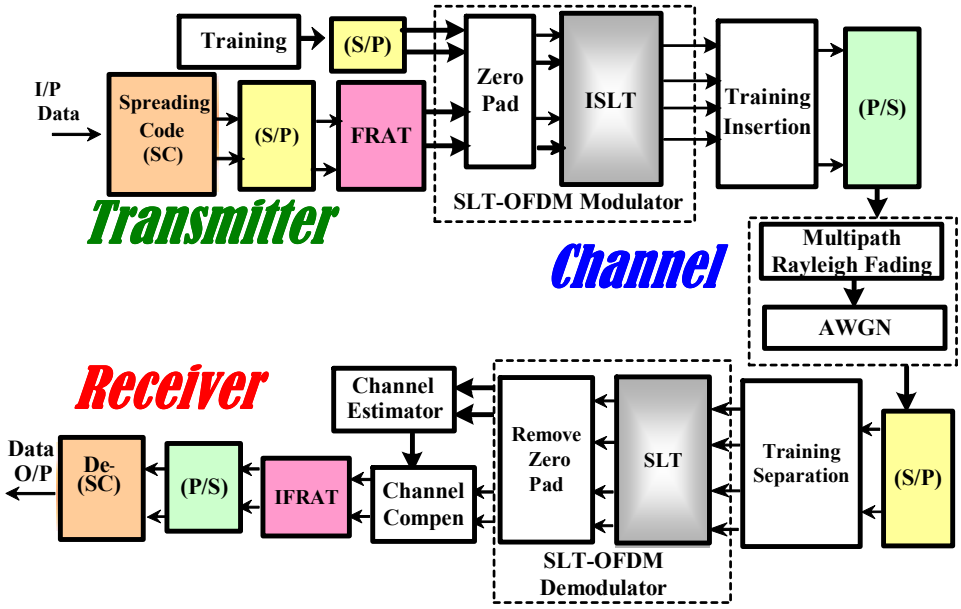

Fig. 6. Block diagram of the proposed Radon-SLT-MC-CDMA system

FRAT is used for mapping the spreading sequences. After that, a pilot-carrier (training sequence), which may be a bipolar sequence $\{\pm 1\}$ previously informed to receiver, is generated. The SLT-OFDM modulator-demodulator works according to the procedure described in [14] and provided in a previous section. The channel frequency response is estimated by using training and received sequences as follows:

$$H(k) = \frac{\text{Re}\, ceived \quad Training \quad Sample \quad (k)}{Transmitte \quad d \quad Training \quad Sample \quad (k)}, k = 0,1,2,... \tag{14}$$

The channel frequency response previously found is used to compensate the channel effects on the data. The estimated data can be found using the following equation:

$$Estimated - data(k) = H^{-1}_{estimate}(k) * \text{Re}\, ceived - data(k), k = 0,1,2,...$$

V. SIMULATION RESULTS AND DISCUSSION OF THE PROPOSED SYSTEM

In this section, the results of bit error performance simulations using MATLAB 7 for Radon-SLT-MC-CDMA are provided and compared with the conventional FFT-MC-CDMA, Radon-MC-CDMA, and DMWT-MC-CDMA under different channel conditions. AWGN channels, flat fading channels (FFC), and multi-path frequency selective Rayleigh distributed with AWGN channels are considered during simulations. The system parameters used in the simulation are as follows: $T_s = 0.1\mu \sec$, FRAT window: 5 by 5, SLT bins = 32, code length $L_C = 25$.

A. Performance of the Proposed Radon-SLT-MC-CDMA System in AWGN Channel

The BER performances of the proposed Radon-SLT-MC-CDMA and the other three MC-CDMA systems in AWGN channel are shown in Fig. 5.

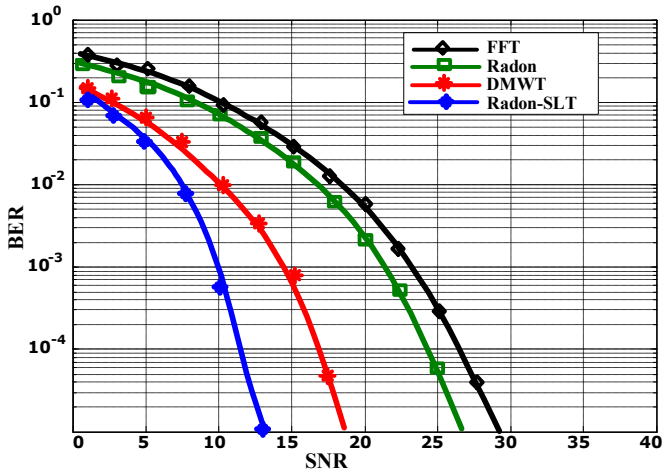

Fig. 5. BER performance of Radon-SLT-MC-CDMA in AWGN channel

From Fig. 5 it can be noted that Radon-SLT-MC-CDMA has a SNR gain of 5dB compared with DMWT-MC-CDMA system, a SNR gain of 13dB compared with Radon-MC-CDMA, and a SNR gain of 16dB compared with FFT-MC-CDMA system to achieve BER of 10-4. This gain improvement achieved increases with decreasing the required BER. Also, it can be concluded that the gain achieved in CDMA when combined with OFDM is better than that achieved in OFDM only because this combination spreads the original data stream using the spreading code and then modulates different carriers with each chip. So, if a comparison is made between gain achieved in Radon-SLT-CDMA and that achieved in Radon-SLT-OFDM, there will be about 8 dB gain.

B. Performance of the Proposed Radon-SLT-MC-CDMA System in Flat Fading Channel with AWGN

In this channel, all signal frequency components are the BER performance of Radon-SLT-MC-CDMA in a 2-ray Rayleigh-distributed multi-path flat fading channel with a second path gain -8dB and a second path delay $\tau_{\max} = 0.1\mu\text{sec}$. It is assumed that all frequency components of the transmitted signal are changed and correlated in phase and magnitude. Five maximum Doppler shifts are used in the simulation: 4Hz, 80Hz, 300Hz, 500Hz, and 1000Hz. The results of simulation are shown in Fig. 8, Fig. 9, Fig. 10, Fig. 11, and Fig. 12.

Fig. 8 shows that BER performance of Radon-SLT-MC-CDMA system is much better than the other systems. It has BER=10-3 at SNR=10dB; DMWT-MC-CDMA has the same BER at SNR=16.5dB; Radon-MC-CDMA has BER=10-3 at SNR=22.5dB; FFT-MC-CDMA system has BER=10-3 at SNR=25dB. This is 6.5dB gain in SNR compared with DMWT-MC-CDMA system, 12.5dB gain compared with Radon-MC-CDMA, and 15dB compared with FFT-MC-CDMA.

Based on the results of simulation, it can be noted that all MC-CDMA systems are sensitive to variations of Doppler shift frequency. However, the proposed system has a minimum sensitivity to variations compared with other systems. Also, it can be noted that the gain achieved by the proposed system increases with increasing Doppler shift frequency compared

with other systems. For the purpose of achieving BER=10-3 at Doppler shift = 1000Hz, the proposed system requires SNR= 15dB, while DMWT-MC-CDMA requires SNR= 27dB, Radon-MC-CDMA requires SNR= 32.5dB, and FFT-MC-CDMA requires SNR= 37.5dB. This is a large gain improvement and an obvious advantage of the proposed system.

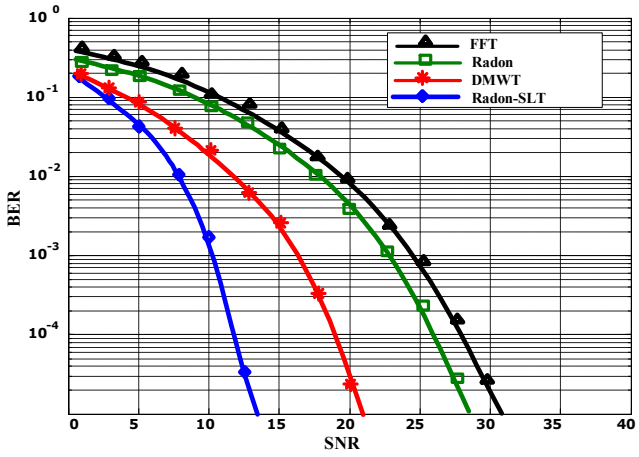

Fig. 8. Performance of Radon-SLT-MC-CDMA in FFC at max. Doppler shift 4Hz

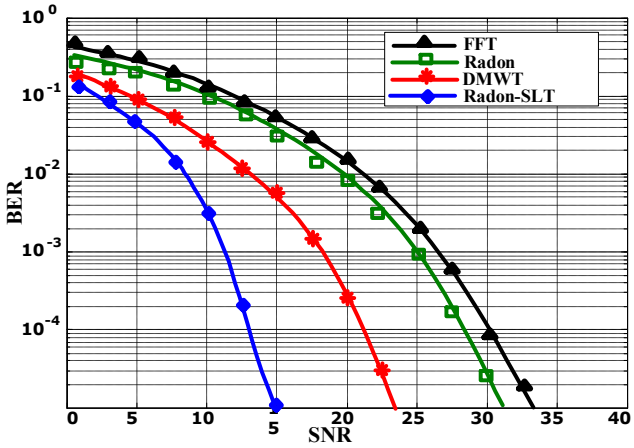

Fig. 9. Performance of the proposed system in FFC at max. Doppler shift 80Hz

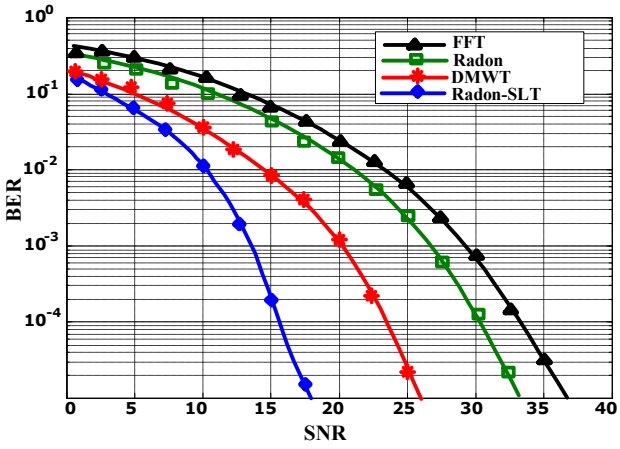

Fig. 10. Performance of the proposed system in FFC at max. Doppler shift 300Hz

C. BER Performance of the Proposed Radon-SLT-MC-CDMA System in Selective Fading Channel with AWGN

In selective fading channel (SFC), the frequency complements of the transmitted signal are affected by uncorrelated changes, where the parameters of the channel correspond to two path systems. For SFC, many models are used in simulation. BER performance is compared to FFT-based, Radon-based, DMWT-based, and Radon-SLT-based MC-CDMA systems. The effect of path attenuation, delay and maximum Doppler shift of an echo was also taken into account. The channel in simulation is assumed to be 2-rays Rayleigh-distributed multi-path fading channel with second path gain -8 dB, and second path delay $\tau_{\max} = 0.1\mu$sec.

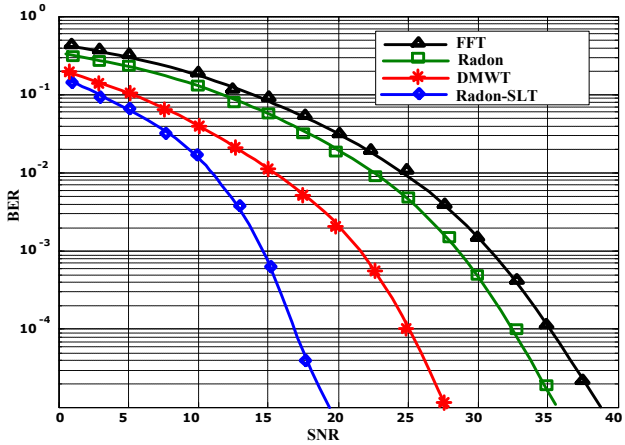

Fig. 11. Performance of the proposed system in FFC at max. Doppler shift 500Hz

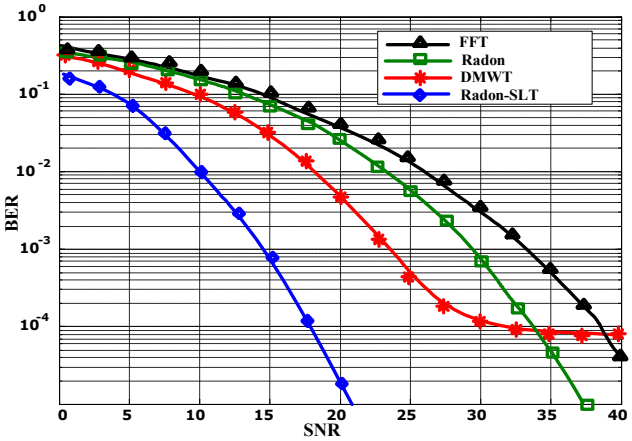

Fig. 12. Performance of the proposed system in FFC at max Doppler shift 1000Hz

Fig. 13 shows the BER performance simulation of the Radon-SLT-MC-CDMA, DMWT-MC-CDMA, Radon-MC-CDMA, and FFT-MC-CDMA systems for a SFC with path delay equal 1 sample, path gain equal -8dB, and Doppler shift equal 4Hz. Fig. 13 shows that BER performance of Radon-SLT-MC-CDMA system is much better than the other systems for such type of channels. The proposed system has BER=10-5 at SNR=16dB; DMWT-MC-CDMA has the same BER at SNR=22.5dB; Radon-MC-CDMA has BER=10-5 at SNR=29dB; FFT-MC-CDMA system has BER=10-5 at SNR=33.5dB. This is 6.5dB gain in SNR compared with DMWT-MC-CDMA system, 13dB gain compared with Radon-MC-CDMA, and 17.5dB gain compared with FFT-MC-CDMA.

Fig. 14, Fig. 15, Fig. 16, and Fig. 17 repeat the BER performance simulation of the four systems for SFC with the same channel parameters except changing Doppler shift to 80Hz, 300Hz, 500Hz, and 1000Hz respectively.

Plots indicate that Radon-DMWT-MC-CDMA system has better performance than DMWT-MC-CDMA, Radon-MC-CDMA, and FFT-MC-CDMA systems. Also, the proposed system is very stable with variations of Doppler frequency in selective fading channels especially when Doppler frequency exceeds 1000 Hz. This is clearly seen in Fig. 16 and Fig. 17 where Doppler frequency equals 300Hz and 500Hz respectively.

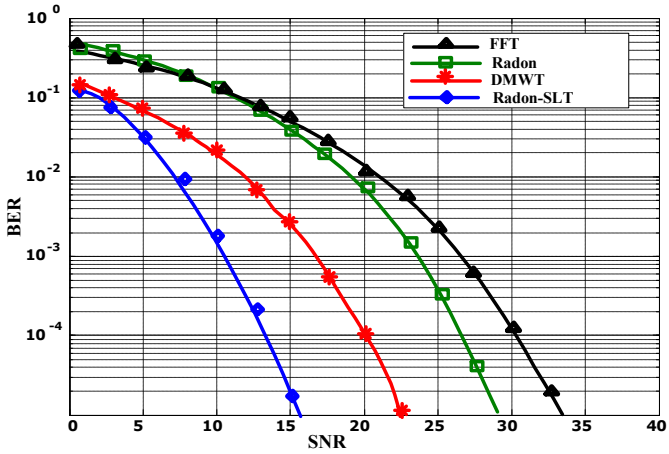

Fig. 13. Performance of the proposed system in SFC at max. Doppler shift 4Hz

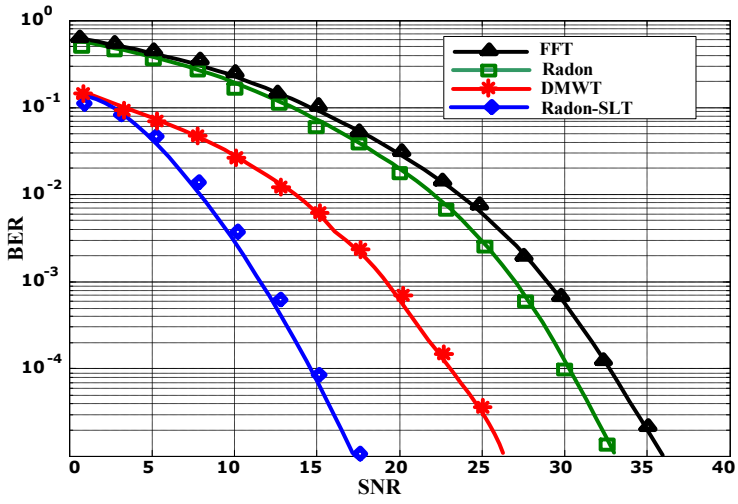

Fig. 14. Performance of the proposed system in SFC at max Doppler shift 80Hz

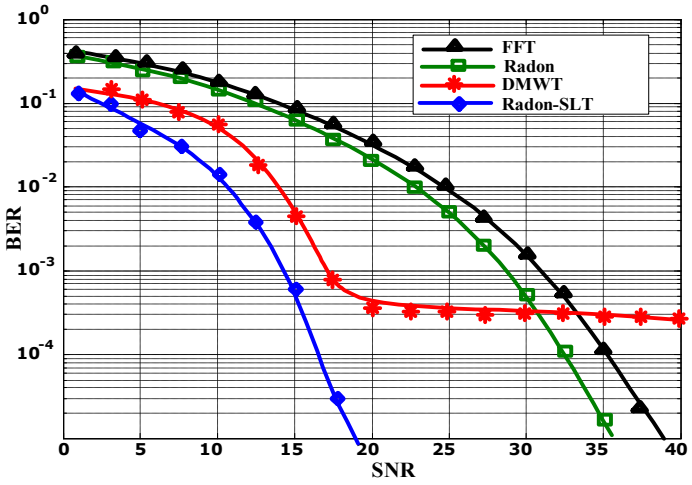

Fig. 15. Performance of the proposed system in SFC at max Doppler shift 300Hz

D. Effect of Channel Parameters Variations on the Performance of the Proposed System

The effect of variations of SFC parameters on the performance of the MC-CDMA systems is very important. It changes the second path gain and delay on the BER performance. Simulations of the effect of the second path gain are made for two cases -12dB and -4dB calculated at Doppler frequency 80Hz and 2nd path delay equal one sample (0.1μsec). The results of BER performance simulations of the four MC-CDMA systems are provided in Fig. 18 and Fig. 19 respectively. These figures show that the proposed system has the smallest sensitivity to the variations of the second path gain and is less affected by it.

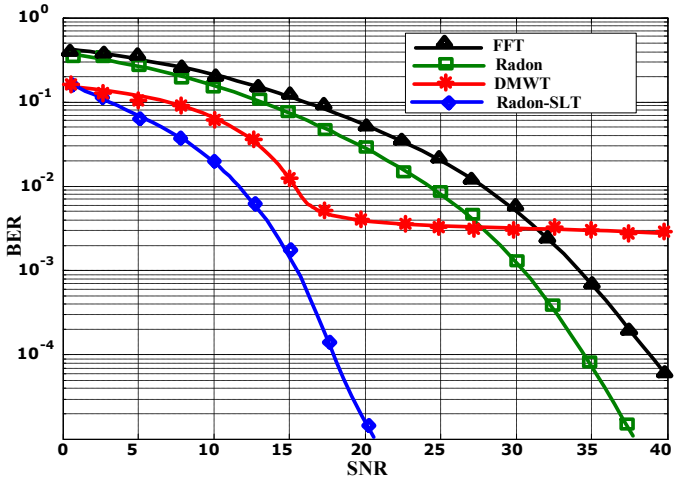

Fig. 16. Performance of the proposed system in SFC at max Doppler shift 500Hz

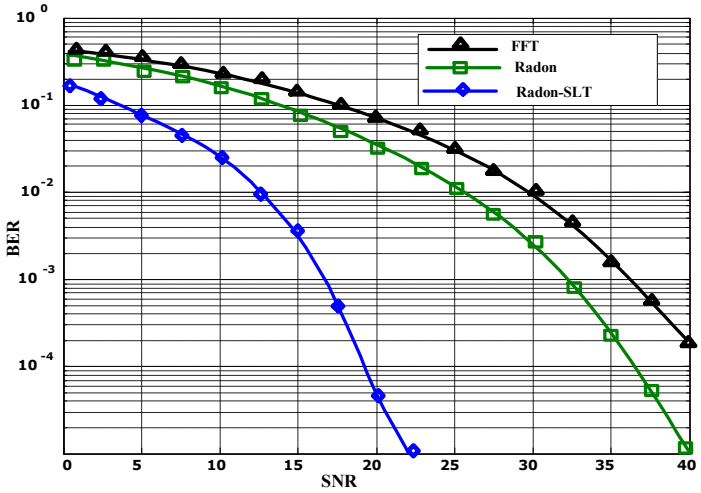

Fig. 17. Performance of the proposed system in SFC at max Doppler shift 1000Hz

The effect of the second path delay of SFC on the BER performance is simulated at Doppler frequency equal 80Hz and second path gain = -8dB for the cases of 10 samples (1μsec). The results of the simulation of the four MC-CDMA systems are shown in Fig. 20. Previously, Fig. 14 provided the simulation for the same channel parameters and for the case of 1 sample (0.1μsec) path delay. The BER simulations of the four systems when changing the second path delay of SFC show that the proposed system has the best performance in all situations.

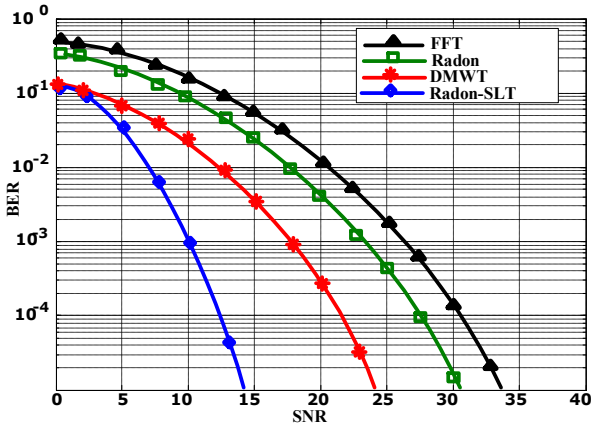

Fig. 18. Performance of the proposed system in SFC with second path gain -12dB

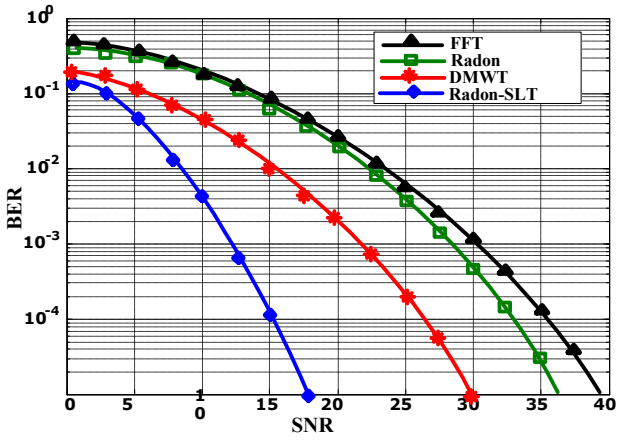

Fig. 19. Performance of Radon-SLT-MC-CDMA in SFC with second path gain -4dB

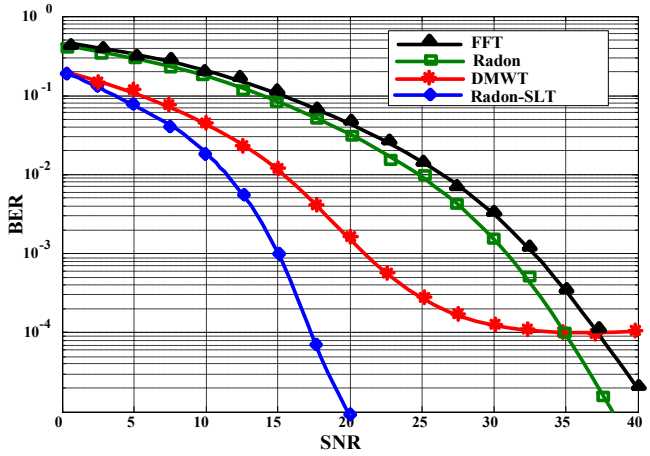

Fig. 20. BER performance of Radon-SLT-MC-CDMA in selective fading Rayleigh channel with path delay equal 10 samples

VI. CONCLUSIONS

In this paper, a novel MC-CDMA system is designed and implemented. Radon-SLT-OFDM transceiver scheme is used in the proposed MC-CDMA system instead of conventional FFT-OFDM. High orthogonal robust to noise interference SLT and FRAT are used to improve the performance of the communication system without a need of using a cyclic prefix which reduces the system complexity and increase the transmission rate as well as spectral efficiency.

Based on the comparison of the performance of Radon-SLT-MC-CDMA, DMWT-MC-CDMA, Radon-MC-CDMA, and FFT-MC-CDMA in AWGN channel, FFC, and SFC, it can be concluded that AWGN channel Radon-SLT-MC-CDMA has performance gain of about 17dB compared with FFT-MC-CDMA to achieve BER = 10-5. For FFC and for different maximum Doppler shift frequencies, Radon-SLT-MC-CDMA system has better performance than all other systems. It has performance gain of about 19dB compared with FFT-MC-CDMA to achieve BER = 10-5at max Doppler shift equal 500Hz. In SFC, the proposed Radon-SLT-MC-CDMA has better performance than DMWT-MC-CDMA, Radon-MC-CDMA, and FFT-MC-CDMA in all cases and for changing all channel parameters. The Proposed system is less affected by changing channel parameters than other systems, while DMWT-MC-CDMA performance is badly affected by max Doppler shift.

It can be noted that CDMA when combined with OFDM has a better BER performance than when using OFDM only. This can be addressed to spread the original data stream then modulate different carriers with each chip.

REFERENCES

[1] E. Biglieri, J. Proakis and S. Shamai, "Fading channels: information-theoretic and communications aspects," *IEEE Transactions on Information Theory,* vol. 44, no. 6, pp. 2619-2692, 1998.

[2] A. H. Kattoush, "A novel radon-wavelet based OFDM system design and simulation under different channel conditions," *International Arab Journal of Information Technology*, vol. 7, no. 4, pp. 416-424, 2010.

[3] A. H. Kattoush, "Radon-DWT MC-CDMA transceiver design and simulation under different channel conditions," *International Arab Journal of Information Technology*, vol. 9, no. 3, pp. 225-234, 2012.

[4] N. H. Tran, H. H. Nguyen and T. Le-Ngoc, "Bit-interleaved coded OFDM with signal space diversity: subcarrier grouping and rotation matrix design," *IEEE Transactions On Signal Processing,* vol. 55, no. 3, pp. 1137–1149, 2007.

[5] V. DaSilva and E. S. Sousa, "Multicarrier orthogonal CDMA codes for quasisynchronous communication systems," *IEEE Journal on Selected Area in Communications*, vol. 12, no. 5, pp. 842-852, 1994.

[6] S. Hara and R. Prasad, "Overview of multicarrier CDMA," *IEEE Communications Magazine*, vol. 35, no. 12, pp. 126-133, 1997.

[7] S. Kondo and L. B. Milstein, "Performance of multicarrier DS CDMA systems," *IEEE Transactions on Communications,* vol. 44, no. 2, pp. 238-246, 1996.

[8] E. A. Sourour and M. Nakagawa, "Performance of orthogonal multicarrier CDMA in a multipath fading channel," *IEEE Transactions on Communications,* vol. 44, no. 3, pp. 356-366, 1996.

[9] L. Vandendorpe, "Multitone spread spectrum multiple access communications system in a multipath rician fading channel," *IEEE Transactions on Vehicular Technology,* vol. 44, no. 2, pp. 327-337, 1995.

[10] N. Yee, J-P. Linnartz and G. Fettweis, "Multicarrier CDMA in indoor wireless radio networks," *Proc. of IEEE PIMRC*, pp. 109-113, 1993.

[11] B. G. Negash and H. Nikookar, "Wavelet based OFDM for wireless channels," *Vehicular Technology Conference,* pp. 688-691, 2001.

[12] I. W. Selesnick, "The slantlet transform," *IEEE Transactions on Signal Processing,* vol. 47, no. 5, pp. 1304-1313, 1999.

[13] S. Agaian, K. Tourshan and J. Noonan, "The fast parametric slantlet transform with applications" Proc. of SPIE, pp. 1-12, 2004.

[14] A. H. Kattoush and M. M. Qasaymeh, "Performance of a slantlet based OFDM transceiver under different channel conditions," *International Journal of Information Technology and Computer Science,* vol. 4, no. 1, pp. 64-72, 2012.

[15] A. H. Kattoush and M. M. Qasaymeh, "Design and Simulation of MC-CDMA Transceiver via Slantlet Transform," *International Journal of Information Technology and Computer Science,* vol. 4, no. 3, pp. 16-23, 2012.

[16] W. Al-Jawhar, A. H. Kattoush, S. M. Abbas and A. T. Shaheen, "A high performance parallel radon based OFDM transceiver design and simulation," *Digital Signal Processing*, vol. 18, no. 6, pp. 907-918, 2008.

[17] A. H. Kattoush, W. A. Al-Jawhar, A. Shaheen and A. Ghodayyah, "The performance of proposed one dimensional serial radon based OFDM system under different channel conditions," *International Journal of Computers, Systems and Signals,* vol. 9, no. 2, pp. 3-16, 2008.

[18] A. H. Kattoush, W. A. Mahmood, S. M. Abbas and A. T Shaheen, "A N-radon Based OFDM trasceivers design and performance simulation over different channel models," *Wireless Personal Communications*, vol. 58, no.4, pp. 695-711, 2011.

[19] A. H. Kattoush, W. M. Al-Jawhar and A. T. Shaheen, "A novel radon-based multi-carrier direct sequence-code division multiple access transceiver design and simulation," *International Journal of Communication Networks and Distributed Systems,* vol. 4, no. 4, pp. 436-452, 2010.

[20] A. H. Kattoush and W. Al-Jawhar, "Multiwavelet computed radon-based OFDM transceiver designed and simulation under different channel conditions," *Journal of Information and Computing Science,* vol. 5, no. 2, pp. 133-145, 2010.

[21] A. H. Kattoush and W. Al-Jawhar, "Wavelet computed radon-based OFDM transceiver designed and simulation under different channel conditions," *Current Development in Theory and Applications of Wavelets,* vol. 5, no. 2-3, pp. 93-118, 2011.

[22] A. H. Kattoush, W. Al-Jawhar and O. Q. Al-Thahab, "A novel radon-multiwavelet based OFDM system design and simulation," *Wireless Personal Communications,* vol. 71, no. 2, pp 857-871, 2013.

[23] A. H. Kattoush, "A radon-slantlet based OFDM system design and performance under different channel conditions," *ISRN Communications and Networking,* vol. 2012, pp. 1-8, 2012.

[24] N. M. Do and M. Vetterli, "The finite ridgelet transform for image representation," *IEEE Transactions on Image Processing,* vol. 12, no. 1, pp. 16-28, 2003.

[25] B. Alpert, G. Beylkin, R. Coifman and V. Rokhlin, "Wavelet-like bases for the fast solution of second-kind integral equations," *SIAM Journal on Scientific Computing,* vol. 14, no. 1, pp. 159-184, 1993.

[26] I. Daubechies, "Ten Lectures on Wavelets," *CBMS-NSF Regional Conference Series in Applied Mathematics,* 1992.

[27] O. Oy, "Channel and delay estimation algorithms for wireless communication systems," Ph.D Thesis, Helsinki University of Technology, Signal Processing Laboratory, Finland, 2003.